RAPID RETROFITTING TECHNIQUES FOR INDUCED EARTHQUAKES

Quarterly Progress Report
For the period ending May 31, 2018

Submitted by:
P. S. Harvey Jr. (PI)
K. K. Muraleetharan (Co-PI)
S. Sivakumaran (Graduate Student)

Affiliation: School of Civil Engineering and Environmental Science
University of Oklahoma
Norman, OK

ABC UTC
ACCELERATED BRIDGE CONSTRUCTION
UNIVERSITY TRANSPORTATION CENTER

Submitted to:
ABC-UTC
Florida International University
Miami, FL

1 Background and Introduction

Since 2009, there has been a dramatic increase in the number of earthquakes in the central U.S. (Fig. 1) [1]. States such as Oklahoma, Kansas, Arkansas, and Texas have not historically experienced earthquakes at the rate currently observed, nor of this magnitude [2]. Studies such as by Keranen et al. [3] have linked the increased rate of seismic activity since 2009 to wastewater injection in disposal wells. These induced earthquakes are not limited to the U.S., but are also experienced in other countries including Canada, China, and the United Kingdom [2]. The seismicity of places such as California and the New Madrid seismic zone is well documented and generally thought of when discussing seismic hazards in the contiguous U.S. Yet the cumulative moment in Oklahoma in 2015 and 2016 (1 January 2015 to 31 December 2016) exceeded that of southern California and the New Madrid seismic zones.

The major fault in the central U.S. is the New Madrid fault [4] located along the Mississippi River between Tennessee, Arkansas, Missouri, and Kentucky. The only other identified source of tectonic earthquakes in this region is the Meer's fault in southwest Oklahoma, as reflected in the U.S. Geological Survey (USGS) national seismic hazard maps [5] and accordingly the mapped design ground motion data provided by design provisions, such as the *2009 AASHTO Guide Specifications for LRFD Seismic Bridge Design* [6]. In 2016, the USGS made an effort to incorporate non-tectonic earthquakes (or "induced seismicity") into the national seismic hazard model [7], but these are not reflected in seismic design provisions. Accordingly, concern has risen about how civil infrastructure in the central U.S. will handle the increased seismic demand.

A majority of the earthquakes occurring in the central U.S. are small-to-moderate in magnitude, ranging from magnitude (M) 3.0 to 5.0. Over the last decade, the central U.S. has experienced nearly 120 M4.0 and greater earthquakes, with a majority (81) occurring in Oklahoma. At 12:02:44 Coordinated Universal Time (UTC) on 3 September 2016, a M5.8 earthquake struck 15 km northwest of Pawnee, Oklahoma. The event was triggered by strike-slip faulting within the interior of the North America plate [8], at a focal depth of 5.6 km and is the largest recorded event in Oklahoma to date. Over the decade prior to this event, the central U.S. experienced two other events larger than M5.0: the 6 November 2011 M5.7 earthquake near Prague, Oklahoma [9] and

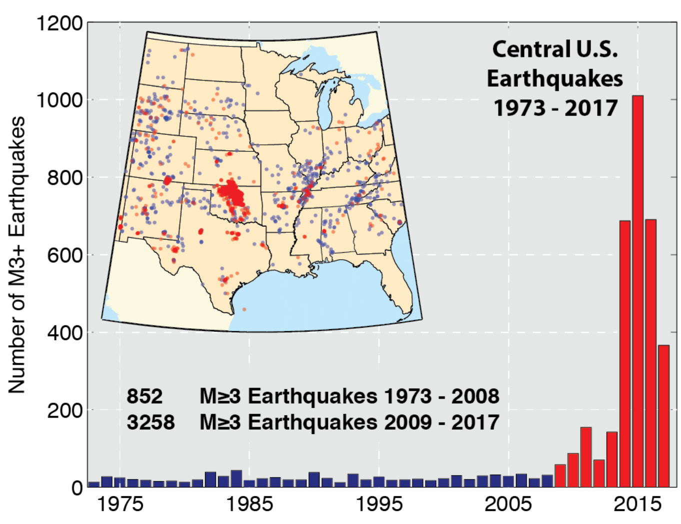

Figure 1: Cumulative number of earthquakes with a magnitude 3.0 or larger in the central United States [1].

the 13 February 2016 M5.1 earthquake near Fairview, Oklahoma [10]. A fourth large event (M5.0) occurred on 7 November 2016 near Cushing, Oklahoma [11]. These M5.0 and larger events were felt in the surrounding states, caused damage to residential structures, and resulted in minor injuries [12]. Slight damage to highway bridges was also reported following the M5.8 Pawnee event, which included spalling of concrete on one bridge [13] and a roller bearing coming dislodged on another (W. L. Peters, *pers. comm.*, 20 October 2016).

While collapse is unlikely for the induced earthquakes currently observed, the cumulative effects of a large number of small earthquakes on bridges are not fully understood. These cumulative effects compounded with the occasional moderate earthquake (M5.0 and larger) may lead to damage requiring rapid repairs to avoid acute traffic control issues at the affected bridge sites. To reduce impacts to the driving public, *accelerated bridge construction* (ABC) techniques have been developed over recent years [14], but have primarily focused on rapidly constructing new or replacement structures. Another benefit derived from these ABC methods is rapid post-earthquake repair of damaged structures. Post-earthquake accelerated column repair/replacement was identified as a high priority research need at a Federal Highway Administration (FHWA) workshop on seismic ABC [15]. While this workshop focused on moderate-to-high seismic zones, the need for additional analysis, new techniques, and associated specifications is also critical for low-to-moderate seismic zones affected by induced earthquakes. This project will address the current knowledge gap on the effects of low-level frequent seismic events on bridges, as well as ABC methods to repair/retrofit damaged bridges.

2 Problem Statement

The recent surge in seismic activity in the central U.S. has motivated the need for rapid repair techniques that leverage ABC methods. The overarching objective of this project is to develop analysis techniques to study the effect of large number of small earthquakes on bridges and identify appropriate ABC methods for repair of bridges damaged by induced earthquakes. The project will use Oklahoma as a case study and develop techniques and tools that can be applied to other regions experiencing low-level frequent seismic events. Ultimately, the research will result in the following outcomes: (a) new seismic analysis tools to assess for damage from repeated, small-to-moderate earthquakes; (b) guidelines for the appropriate use of these tools; (c) specifications for the application of ABC repair methods in practice.

3 Research Approach and Method

The overall approach of this project is organized in two phases: (I) Seismic Hazard Characterization and (II) ABC Repair Guidelines. Phases I and II will be performed in a linear consecutive fashion, with each phase requiring one year. Phase I, which is the focus of this report, involves seismic hazard analysis, numerical modeling, response prediction, and guideline development. Oklahoma and the surrounding area — a region experiencing large numbers of small-to-moderate earthquakes — serves as the testbed for this project. The following section provides additional detail on the tasks that have been, and will be, performed to achieve the project objective in Year 1 of this 2-year project.

4 Description of Research Project Tasks

The following is a description of tasks carried out to date.

4.1 Task 1 – Compile Ground-Motion Data

Description: *The first task of this project is to compile ground-motion data for earthquakes impacting Oklahoma's bridges. In addition to the processed ground-motion time histories, key ground-motion intensity measures, such as peak ground acceleration (PGA), peak ground velocity (PGV), and the 5%-damped spectral acceleration (PSA), will be compiled. Metadata, such as station longitude/latitude, soil conditions, channels, etc., will be curated as well.*

This first objective of this task was to identify the time frame, seismic stations, and earthquakes that would comprise the ground-motion data set. As seen in Fig. 1, the number of M3 and larger earthquakes has progressively increased in recent years. Fig. 2 portrays the temporal and spatial variation in seismic activity over 5-year periods: (a) 2003–2007, (b) 2008–2012, and (c) 2013–2017. Clearly the number of earthquakes has skyrocketed in the last five years. While the highest number of earthquakes was recorded in 2015 (nearly 950 in Oklahoma alone), 2016 was marked by larger magnitude events: twenty-one M $\geq$ 4.0 earthquakes, including three M $\geq$ 5.0 earthquakes. Therefore, the one-year time frame 1 January 2016 to 31 December 2016 was selected for this study.

The seismicity in Oklahoma has been concentrated in the north-central portion of the state in recent years (see Fig. 2(c)). Seismic stations OK.U32A and GS.OK005 were identified as being close in proximity to the recent seismic activity, as well as being active the entire year. Table 1 presents these stations, their locations and soil conditions (V_{s30}), as well as which horizontal channels are of interest. OK.U32A is close to Fairview in northwest Oklahoma, and GS.OK005 is northeast of Oklahoma City, so these stations capture different regions of seismic activity across

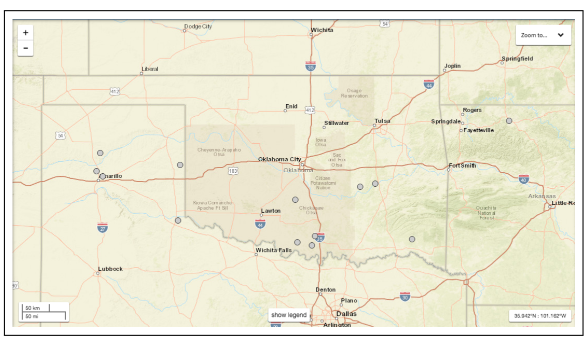

(a) 2003–2007

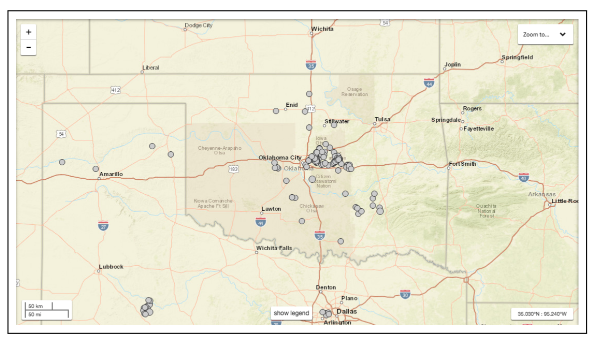

(b) 2008–2012

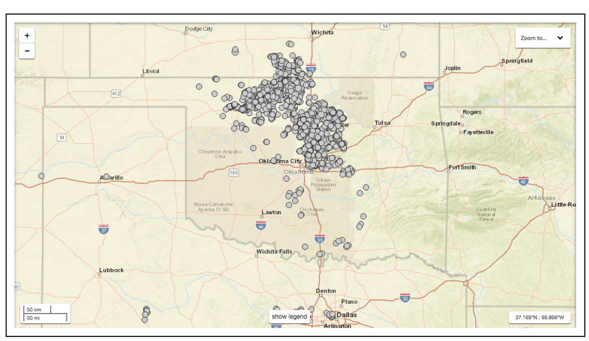

(c) 2013–2017

Figure 2: Magnitude 3.0 and larger earthquakes in Oklahoma [16]: (a) 2003–2007 ($\approx$ 12 events), (b) 2008–2012 ($\approx$ 164 events), and (b) 2013–2017 ($\approx$ 2634 events).

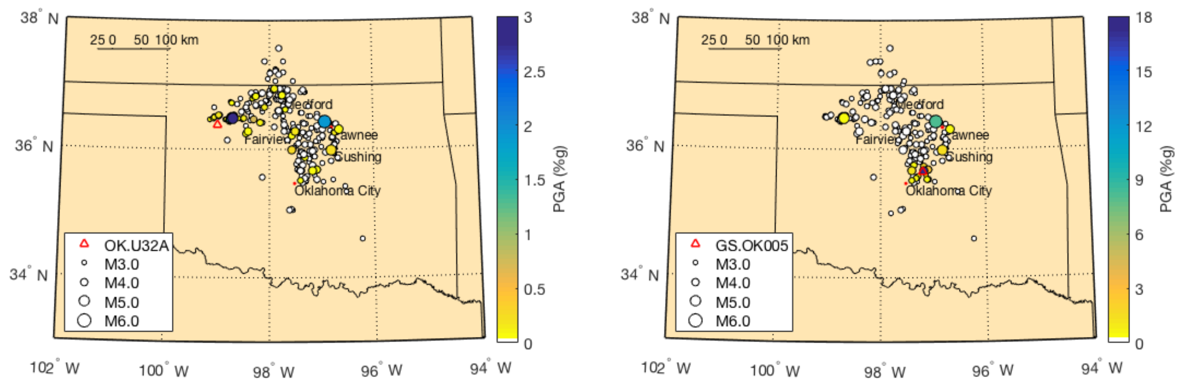

(a) OK.U32A

(b) GS.OK005

Figure 3: Seismic stations and earthquakes in the ground-motion data set.

the state. The ground-motion accelerograms captured by these stations will be used to represent the seismic activity a bridge close to these stations would have been exposed to during the one-year period (2016).

Ground-motion records were retrieved from Standing Order for Data (SOD) [18] for the two stations for all M3.0 and larger earthquakes during the time frame of interest. Bidirectional ground motions are considered, so both the East and North components were retained, but the vertical components were not included. The records were processed following the PEER processing procedure [19]. A total of 614 and 424 earthquakes were processed for the two stations, respectively. Fig. 3 shows the locations of these earthquakes with respect to the seismic stations. The marker size indicates the magnitude of the event, and the marker face color indicates the peak ground acceleration (PGA) measured by the particular station, discussed below.

The second objective of this task was to compile key ground-motion intensity measures. Of particular interest are PGA and spectral acceleration S_a. The PGA shown in Fig. 3 is the largest acceleration in any direction:

$$\mathrm{PGA} = \max_t \sqrt{[\ddot{u}_{g1}(t)]^2 + [\ddot{u}_{g2}(t)]^2} \tag{1}$$

where $\ddot{u}_{g1}(t)$ and $\ddot{u}_{g2}(t)$ are the ground accelerations in two orthogonal horizontal directions, in this case East and North. Fig. 4 shows these PGA values versus the epicentral distance to get a sense of ground-motion attenuation with distance from the epicenter. As expected, stronger shaking is observed for earthquakes closer to the station. Larger magnitude events tend to produce stronger

Table 1: Seismic stations composing the ground-motion suite.

Station	Latitude	Longitude	V_{s30}^* (m/s)	Channel	
				East	North
OK.U32A	36.3795	−99.0014	575	BHE	BHN
GS.OK005	35.6549	−97.1911	518	HNE	HNN

* V_{s30} values were taken from [17]

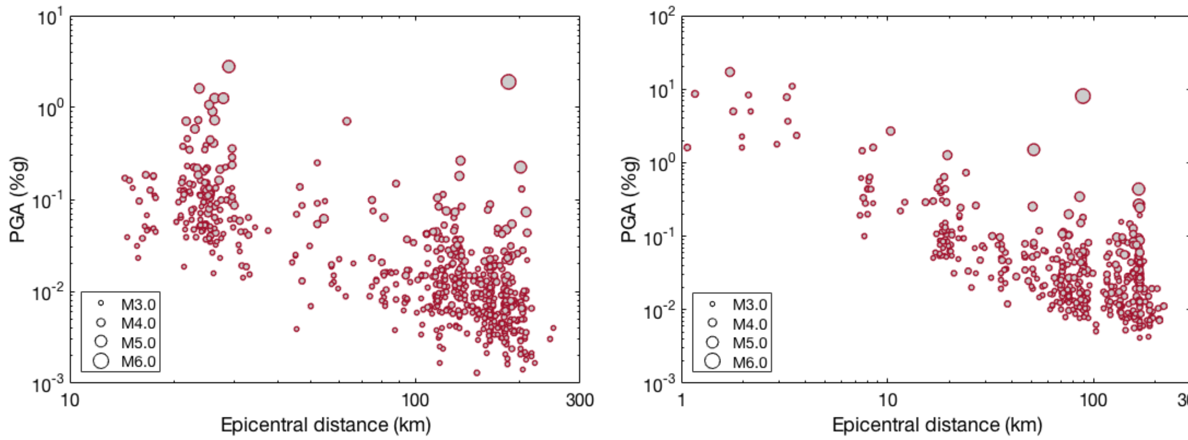

(a) OK.U32A (b) GS.OK005

Figure 4: Attenuation of peak ground acceleration (PGA) with epicentral distance from seismic stations (a) OK.U32A and (b) GS.OK005.

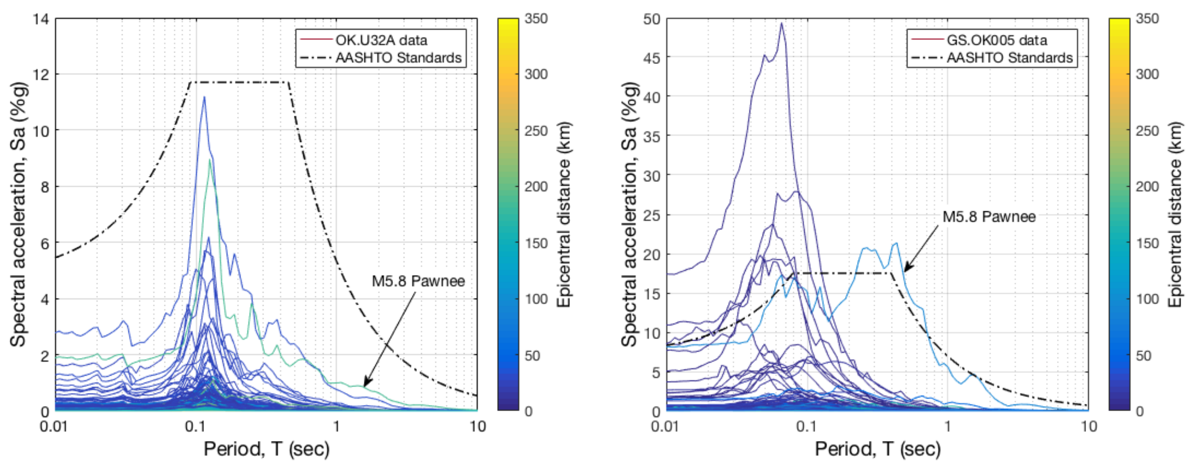

(a) OK.U32A (b) GS.OK005

Figure 5: Spectral response acceleration S_a (5% damped) measured at seismic stations compared with the design response spectra per the *2009 AASHTO Guide specifications for LRFD seismic bridge design* [6]: (a) OK.U32A and (b) GS.OK005.

shaking. Notably, the M5.8 Pawnee event produces some of the largest shaking even though it occurred farther from the stations than some of the smaller events.

Spectral accelerations are of particular interest to structural engineers. Fig. 5 shows the response spectra for all the earthquakes measured at (a) OK.U32A and (b) GS.OK005. The spectral acceleration reported is the largest radial acceleration:

$$S_a(T) = \max_t \sqrt{[a_1(t;T)]^2 + [a_2(t;T)]^2} \tag{2}$$

where $a_1(t;T)$ and $a_2(t;T)$ are the 5%-damped acceleration responses in two orthogonal horizontal directions for a structure with period T. This is an orientation-independent measure of the spectral acceleration, as opposed to the geometric mean of the response spectra in the two directions [20].

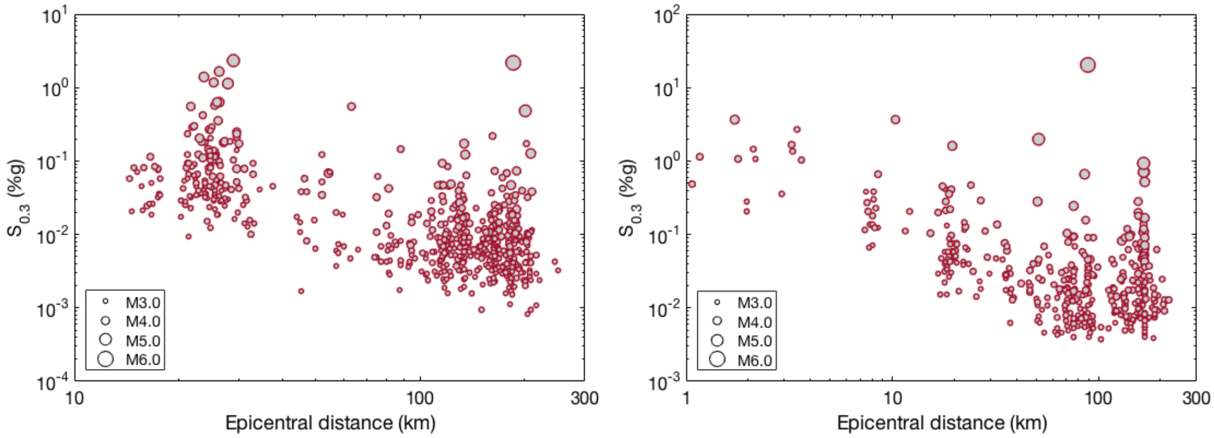

(a) OK.U32A (b) GS.OK005

Figure 6: Attenuation of 0.3-sec spectral acceleration ($S_{0.3}$) with epicentral distance from seismic stations (a) OK.U32A and (b) GS.OK005.

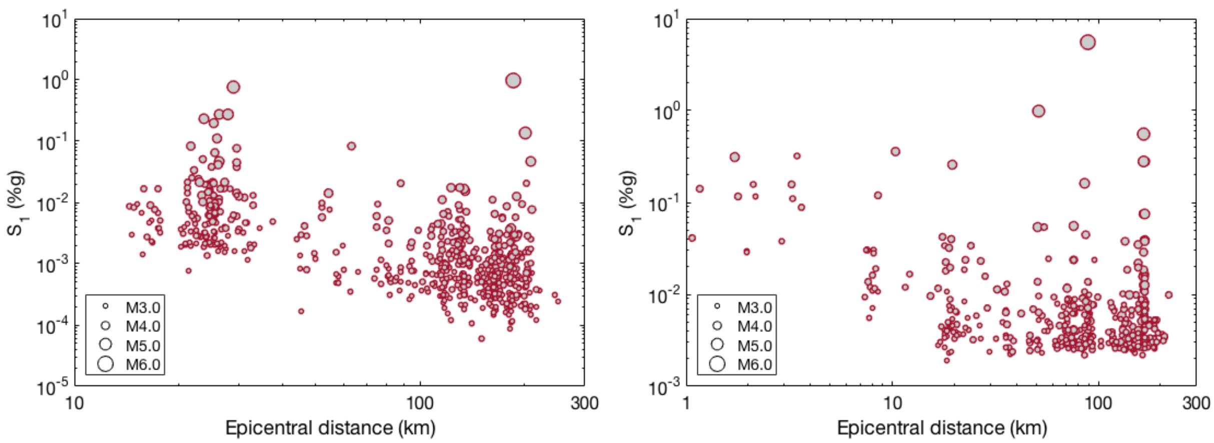

(a) OK.U32A (b) GS.OK005

Figure 7: Attenuation of 1-sec spectral acceleration ($S_{0.3}$) with epicentral distance from seismic stations (a) OK.U32A and (b) GS.OK005.

The largest spectral accelerations are observed at periods between 0.05 and 0.3 seconds. There is variation in the response spectra due to magnitude of the event and distance from the epicenter. To illustrate the latter, the measured response spectra in Fig. 5 are color coded according to their epicentral distance. In general the spectral accelerations decrease with increasing epicentral distance (i.e., attenuate). The attenuation of spectral accelerations at 0.3 and 1.0 sec ($S_{0.3}$ and S_1, respectively) with epicentral distance is shown in Figs. 6 and 7, respectively.

Fig. 5 also shows the design response spectra per the *2009 AASHTO Guide specifications for LRFD seismic bridge design* [6] as a point of comparison for the spectral acceleration from each station. The design spectra assume site class C based on the shear wave velocity determined at the seismic station (Table 1). Because the design curves are based on the hazard from the Meers fault in southwest Oklahoma, the design spectral accelerations are higher closer to the fault (GS.OK005) and lower farther from the fault (OK.U32A). However, as can be seen from Fig. 5, this does not necessarily correspond to the intensity of the ground motions from the recorded earthquakes.

In summary, two seismic stations (OK.U32A and GS.OK005) were identified for this Oklahoma case study that will consider M3.0 and larger earthquakes in 2016. Over 1000 bidirection accelerograms were acquired and processed, extracting intensity measures (PGA and S_a) of interest to bridge analysis and design. The data collected in this task will be used in Task 2 to quantify cumulative demand due to induced earthquakes.

4.2 Task 2 – Characterize Cumulative Seismic Demand

Description: *This task will use ground-motion data acquired in Task 1 to quantify the cumulative (or cyclic) seismic demand due to induced earthquakes. OpenSees models of typical Oklahoma bridges will be used to run simulations and to determine the number of cycles, and the amplitude of these cycles, that Oklahoma bridges were subjected to over the period of highest seismic activity (2013–2017).*

Work performed on Task 2 includes preliminary processing the data compiled in Task 1 to extract cyclic demand statistics. Peak intensity measures, such as PGA and S_a, are critical when determining the largest loads a bridge may experience, but of interest to this project is the number of stress cycles, and fluctuations, Oklahoma bridges have been subjected to in recent years. For the levels of shaking observed, the responses are expected to primarily remain in the *elastic* range, but may compromise durability due to fatigue and weaken the structure when subsequently shaken by larger events (M ≥ 5.0 earthquakes). In Task 2, first a literature review was performed to determine the state of practice in fatigue analysis.

Fatigue is the weakening of a material caused by repeated applied loads. Fatigue occurs at stress values much less than the yield or ultimate strength of the material. Material performance is commonly characterized by an S-N curve, which represents the number of cycles to failure, N, for a given magnitude of cyclic stress, S. These curves assume repeated cycles at the same cyclic stress magnitude. This assumption is not valid when considering bridges subjected to repeated seismic loads. That is, the amplitude of cycles will vary considerably during a single event, as well as under different events of different magnitude located at different distances from the bridge. Therefore, a spectrum of stress magnitudes, S_i ($i = 1, 2, ..., k$), is expected, each contributing n_i cycles. Each of these stress magnitudes has a corresponding number of cycles to failure, $N_i(S_i)$. The most popular method to account for the spectrum of stresses and number of cycles is *Miner's Rule* [21]:

$$C = \sum_{i=1}^{k} \frac{n_i}{N_i} \tag{3}$$

where the material will fail in fatigue when the damage fraction, C, equals 1. The interpretation of Miner's rule is that the proportion of the life consumed at each stress level, n_i/N_i ($i = 1, 2, ..., k$), linearly combine with one another. Note that Miner's rule does not take into account the order in which the cyclic loads are applied.

An approach based on Miner's rule will be assumed in this work. This requires counting the number of cycles a bridge is subjected to when excited by a sequence of earthquakes. The standard practice for cycle counting in fatigue analysis is *rainflow counting* [22], originally proposed by Matsuishi and Endo in 1968 [23]. Rainflow counting will be used to quantify the cyclic demand on bridges.

Preliminary work will consider a simple harmonic oscillator subjected to the sequence of earthquake ground motions acquired in Task 1. A 5%-damped, single-degree-of-freedom oscillator with varying natural period T will be analyzed, similar to the concept used to generate response spectra. The displacement cycles will be counted using the rainflow counting method implemented in Matlab based on the ASTM standard procedure.

Ongoing work to be performed on Task 2 includes selecting a typical Oklahoma bridge that will be modeled in *OpenSees* [24]. This bridge will be subjected to the earthquake sequences to characterize the stress cycles on the RC columns to assess for fatigue.

4.3 Task 3 – Develop and Evaluate a Fatigue Damage Index

Description: *This task will use the cumulative seismic demand found in Task 2 to develop a fatigue damage index (FDI). The FDI will be used to capture structural deterioration due to accumulated seismic damage by quantifying how close a bridge is to its fatigue limit for a given earthquake sequence, from which the remaining service life can be determined.*

4.4 Task 4 – Prepare Guidelines and Final Report

Description: *The project findings from the previously identified tasks will be prepared by means of a final report. The report will include guidelines for the appropriate use of the FDI developed in Task 3.*

5 Expected Results and Specific Deliverables

The two major deliverables from year 1 of this 2-year project are:

- Deliverable 1: Induced Earthquake Ground-Motion Database

  An immediate outcome of Phase I of this project will be a database of ground-motion data from induced earthquakes in Oklahoma. These data and metadata compiled through Task 1 will be made publicly available to allow other researchers to use the data. This data will have practical applications to other projects related to ground-motion modeling, induced seismic hazard forecasting, among others.

- Deliverable 2: Tentative ABC-UTC Guidelines for Assessing Effect of Frequent, Low-Level Seismic Events

  The primary deliverable of Phase I is the guidelines for application of the fatigue damage index (FDI). These guidelines will serve as a valuable tool for practitioners to assess cumulative damage in bridge columns, as well as evaluate the remaining structural capacity of in-service bridges. The guidelines will be developed so as to be easily adopted by state DOTs impacted by induced earthquakes. We anticipate that these guidelines will directly interface with the guidelines to be developed in Phase II for the rapid repair of damaged structural elements with ABC techniques.

6 Schedule

Progress of tasks in year 1 of this project is shown in Table 2.

Table 2: Project schedule.

Phase	Research Task	2018											
		J	F	M	A	M	J	J	A	S	O	N	D
I	1. Compile Ground-Motion Data	Work Performed	Work Performed	Work Performed									
	2. Characterize Cumulative Seismic Demand			Work Performed	Work Performed	Work Performed	Work to be Performed						
	3. Develop and Evaluate a Fatigue Damage Index						Work to be Performed	Work to be Performed	Work to be Performed	Work to be Performed	Work to be Performed	Work to be Performed	
	4. Prepare Guidelines and Final Report										Work to be Performed	Work to be Performed	Work to be Performed

Work Performed   Work to be Performed

7 References

[1] USGS, Induced earthquakes, *Earthquake Hazards Program*, U. S. Geological Survey, accessed February 17, 2017 (2017).
URL https://earthquake.usgs.gov/research/induced/overview.php

[2] A. McGarr, B. Bekins, N. Burkardt, J. Dewey, W. E. P. Earle, S. Ge, S. Hickman, A. Holland, J. R. E. Majer, A. Sheehan, Coping with earthquakes induced by fluid injection, Science 347 (6224) (2015) 830–831. `doi:10.1126/science.aaa0494`.

[3] K. M. Keranen, H. M. Savage, G. A. Abers, E. S. Cochran, Potentially induced earthquakes in Oklahoma, USA: Links between wastewater injection and the 2011 Mw 5.7 earthquake, Geology 41 (6) (2013) 699–702. `doi:10.1130/G34045.1`.

[4] A. D. Frankel, D. Applegate, M. P. Tuttle, R. A. Williams, Earthquake hazard in the New Madrid Seismic Zone remains a concern, u.S. Geological Survey Fact Sheet: 2009-3071, 2 p (2009).

[5] M. Petersen, M. Moschetti, P. Powers, C. Mueller, K. Haller, A. Frankel, Y. Zeng, S. Rezaeian, S. Harmsen, O. Boyd, N. Field, R. Chen, K. Rukstales, N. Luco, R. Wheeler, R. Williams, A. Olsen, Documentation for the 2014 update of the United States national seismic hazard maps, Tech. Rep. Open-File Report 2014-1091, U. S. Geological Survey (2014).

[6] AASHTO, Guide Specifications for LRFD Seismic Bridge Design, American Association of State Highway and Transportation Officials (AASHTO), Washington D.C. (2009).

[7] M. D. Petersen, C. S. Mueller, M. P. Moschetti, S. M. Hoover, A. L. Llenos, W. L. Ellsworth, A. J. Michael, J. L. Rubinstein, A. F. McGarr, K. S. Rukstales, 2016 one-year seismic hazard forecast for the central and eastern united states from induced and natural earthquakes, Open-File Report 2016-1035, U.S. Geological Survey, Reston, Virginia (2016).

[8] USGS, M 5.8 - 14km NW of Pawnee, Oklahoma, *Earthquake Hazards Program*, U. S. Geological Survey, available at http://earthquake.usgs.gov/earthquakes/eventpage/us10006jxs#executive, accessed 28 November 2016 (2016).
URL http://earthquake.usgs.gov/earthquakes/eventpage/us10006jxs#executive

[9] USGS, M 5.7 - Oklahoma, *Earthquake Hazards Program*, U. S. Geological Survey, available at http://earthquake.usgs.gov/earthquakes/eventpage/usp000jadn#executive, accessed 28 November 2016 (2016).
URL http://earthquake.usgs.gov/earthquakes/eventpage/usp000jadn#executive

[10] USGS, M 5.1 - 31km NW of Fairview, Oklahoma, *Earthquake Hazards Program*, U. S. Geological Survey, available at http://earthquake.usgs.gov/earthquakes/eventpage/us20004zy8#executive, accessed 28 November 2016 (2016).
URL http://earthquake.usgs.gov/earthquakes/eventpage/us20004zy8#executive

[11] USGS, M 5.0 - 3km W of Cushing, Oklahoma, *Earthquake Hazards Program*, U. S. Ge-

ological Survey, available at http://earthquake.usgs.gov/earthquakes/eventpage/us100075y8#executive, accessed 22 December 2016 (2016).
URL http://earthquake.usgs.gov/earthquakes/eventpage/us100075y8#executive

[12] J. Taylor, M. Celebi, A. Greer, E. Jampole, A. Masroor, S. Melton, D. Norton, N. Paul, E. Wilson, Y. Xiao, M5.0 Cushing, Oklahoma, USA earthquake on November 7, 2016, Tech. Rep. Oklahoma-EERI-Recon-Report-2017-02-15-Finalized, EERI (2017).

[13] GEER, The Geotechnical Aspects of the September 3, 2016 M5.8 Pawnee, Oklahoma Earthquake, Tech. rep., Geotechnical Extreme Events Reconnaissance (GEER) (October 17 2016).

[14] M. P. Culmo, Accelerated bridge construction-experience in design, fabrication and erection of prefabricated bridge elements and systems, Tech. Rep. FHWA-HIF-12-013, Federal Highway Administration, Washington, DC (2011).

[15] FHWA, 2007 FHWA Seismic Accelerated Bridge Construction Workshop Outcomes and Follow-up Activities, Tech. rep., Federal Highway Administration, San Diego, CA, Final Report from the Rapid Bridge Construction: Seismic Connections Moderate-to-High Seismic Zones (October 11 2007).

[16] USGS, Latest earthquakes, Online, accessed December 20, 2015 (2017).
URL http://earthquake.usgs.gov/earthquakes/map/

[17] USGS, Custom v_s^{30} mapping, accessed June 18, 2015 (2010).
URL http://earthquake.usgs.gov/hazards/apps/vs30/custom.php

[18] T. J. Owens, H. P. Crotwell, C. Groves, P. Oliver-Paul, SOD: Standing Order for Data, Seismological Research Letters 75 (2004) 515–520. doi:10.1785/gssrl.75.4.515-a.

[19] D. M. Boore, A. Azari Sisi, S. Akkar, Using pad-stripped acausally filterd strong-motion data, Bulletin of the Seimological Society of America 102 (2) (2012) 751–760. doi:10.1785/0120110222.

[20] D. Boore, J. Watson-Lamprey, N. Abrahamson, Orientation-independent measures of ground motion, Bulletin of the Seismological Society of America 96 (4A) (2006) 1502–1511.

[21] M. A. Miner, Cumulative fatigue damage, Journal of Applied Mechanics 12 (1945) A 159–A 164.

[22] ASTM E1049-85(2017), Standard practices for cycle counting in fatigue analysis, ASTM International (2017).

[23] M. Matsuishi, T. Endo, Fatigue of metals subjected to varying stress, in: Japan Society of Mechanical Engineers, 1968.

[24] S. Mazzoni, F. McKenna, M. H. Scott, G. L. Fenves, et al., OpenSees Command Language Manual (July 2007).
URL http://opensees.berkeley.edu/OpenSees/manuals/usermanual/